Front. Earth Sci. 2019, 13(4): 829–835
https://doi.org/10.1007/s11707-019-0771-y

RESEARCH ARTICLE

Cloud type identification for a landfalling typhoon based on millimeter-wave radar range-height-indicator data

Zhoujie CHENG[1,2], Ming WEI (✉)[1], Yaping ZHU[3], Jie BAI[2], Xiaoguang SUN[4], Li GAO[5]

1 Collaborative Innovation Center on Forecast and Evaluation of Meteorological Disasters, Nanjing University of Information Science & Technology, Nanjing 210001, China
2 Beijing Institute of Aviation Meteorology, Beijing 100085, China
3 Beijing Marine Hydrometeorologic Centre, Beijing 100071, China
4 Beijing Meteorological Centre, Beijing 100038, China
5 Taizhou Meteorological Bureau of Zhejiang Province, Taizhou 317000, China

Abstract As a basic property of cloud, accurate identification of cloud type is useful in forecasting the evolution of landfalling typhoons. Millimeter-wave cloud radar is an important means of identifying cloud type. Here, we develop a fuzzy logic algorithm that depends on radar range-height-indicator (RHI) data and takes into account the fundamental physical features of different cloud types. The algorithm is applied to a ground-based Ka-band millimeter-wave cloud radar. The input parameters of the algorithm include average reflectivity factor intensity, ellipse long axis orientation, cloud base height, cloud thickness, presence/absence of precipitation, ratio of horizontal extent to vertical extent, maximum echo intensity, and standard variance of intensities. The identified cloud types are stratus (St), stratocumulus (Sc), cumulus (Cu), cumulonimbus (Cb), nimbostratus (Ns), altostratus (As), altocumulus (Ac) and high cloud. The cloud types identified using the algorithm are in good agreement with those identified by a human observer. As a case study, the algorithm was applied to typhoon Khanun (1720), which made landfall in south-eastern China in October 2017. Sequential identification results from the algorithm clearly reflected changes in cloud type and provided indicative information for forecasting of the typhoon.

Keywords landfalling typhoon, identification of cloud type, millimeter-wave cloud radar, RHI data, fuzzy logic

Received April 2, 2019; accepted June 10, 2019

E-mail: wm_nuist@126.com

1 Introduction

Forecasting of typhoons is an important part of aviation meteorological services, as typhoons can have a great impact on the air transport industry. Judging whether a typhoon is strengthening or weakening is an essential step in typhoon forecasting. As a basic property of cloud, cloud type reflects the present status of a typhoon and its likely evolution. Therefore, accurate identification of cloud type is important in typhoon forecasting.

In operational aviation meteorological services, human visual observations remain the dominant approach to cloud classification (World Meteorological Organization, 2017). Although progress has been made in cloud classification using remote sensing data from satellites and radar, the classification results might be not suitable for operational observations in aviation meteorological services. Sassen and Wang (2008) reported that the lack of cloud vertical profile information is the main factor hindering cloud type identification using passive observations. In recent decades, the application of millimeter-wave cloud radar has led to a new field of cloud-precipitation research (e.g. Kollias et al., 2007; Chu et al., 2017; Chuang and Ayers, 2017; Küchler et al., 2017; Zbyněk et al., 2018; Ashish et al., 2019). Wang and Sassen (2001) used ground-based facilities to identify cloud type and established a role-based classification method that was applied to CloudSat Cloud Profiling Radar (CPR) (Stephens et al., 2002) cloud classification products. A fuzzy logic identification technique was employed in a subsequent cloud classification product (Jet Propulsion Laboratory, 2012). CloudSat/CPR-based studies have demonstrated the capability of millimeter-wave cloud radars for cloud type identification. This is an important advance, as the short-term evolution

of cloud depends on cloud thermodynamic processes, which can be inferred from vertical sections but can be ambiguous in horizontal sections. In this paper, we report a fuzzy logic algorithm developed to automatically classify cloud type based on ground-based Ka-band millimeter-wave cloud radar range-height-indicator (RHI) data. The algorithm is used to analyze temporal changes in the local cloud type in a case study of typhoon Khanun as it made landfall in south-eastern China.

2 Study site and data

We used RHI measurements from a ground-based Ka-band dual-polarized cloud radar located at Zhangzhou (24.52°N, 117.65°E), Fujian Province, south-eastern China. The main parameters of the radar are listed in Table 1.

Table 1 Main parameters of the millimeter-wave cloud radar used in this study

Parameter	Value
Regime	dual-polarized pulse Doppler
Polarization	slant 45° linear polarized emission, co-polar and cross-polar receiver
Frequency	35 GHz
Scanning mode	RHI, PPI, volume scan, stationary direction
Measurements	reflectivity, Doppler velocity, spectral width, linear depolarization ratio
Range	0.15–30 km
Azimuth	0–360°
Elevation	0–90°
Reflectivity	−50 to + 30 dBZ
Velocity	−8.5 to + 8.5 m/s
Spectral width	0–4 m/s
Linear depolarization ratio	−5 to −30 dB

3 Methods

3.1 Cloud clustering analysis

Before classifying cloud type from radar echoes, cloud clusters should be identified. We refer to the scheme used in weather radar studies to identify storms. Multiple thresholds and mathematical morphology modification techniques are used in cloud clustering (Han et al., 2009), which employs the following steps.

1) Quality control of data. A medium filter approach is used to eliminate noise and smooth the data.

2) Gridding of data. Bilinear interpolation is used to form gridded data and to transform data from polar to rectangular coordinates.

3) Digitization of the data using a threshold. The echo data need to be retained where possible, since the identification targets are cloud rather than storm. A lower threshold of the reflectivity factor is used to define reliable data. In this work, we use a value of −25 dBZ.

4) For the digitized data, multiple threshold identifications and mathematical morphology modification are applied to identify cloud clusters. The relevant features of each cloud cluster are calculated, including the average intensity, maximum intensity, height with maximum intensity, intensity standard variance, centroid location, locations of boundary points, average base height, average top height, average thickness, maximum top height, minimum base height, and morphological parameters.

After the above steps are completed, cloud clusters can be quantitatively identified in echo images so that the classified objects are well defined. The features are then applied as inputs to the fuzzy logic algorithm.

3.2 Classification method

A fuzzy logic algorithm is employed for cloud classification. Liu and Chandrasekar (2000) provided an outline of the application of fuzzy logic in classifying hydrometeor type based on polarimetric radar measurements.

3.2.1 Membership function

A beta function is chosen as the membership function, defined as

$$P(x,m,a,b) = \frac{1}{1+\left(\frac{x-m}{a}\right)^{2b}}, \quad (1)$$

where x is the input variable and P is the output variable ranging from 0 to 1, which indicates the probability of a certain mode (herein, cloud type). The three parameters that define the shape of a beta function are its center m, width a, and slope b.

3.2.2 Inputs and outputs

The macro-scale features of cloud include base height, top height, horizontal extent, vertical extent, and water content, as described previously for various cloud types. Wang and Sassen (2001) summarized previous work in this area and conducted a statistical analysis focusing on the thickness characteristics of different cloud types. Previous studies of cloud features (Li et al., 2018; Rodrigo et al., 2018; Wang et al., 2018) provide a useful reference for establishing a fuzzy logic scheme.

Cloud microphysical features, including droplet size, concentration, and phase, are indicated in millimeter-wave cloud radar measurements through their influence on reflectivity. There are notable differences in the distributions of reflectivity among cloud types. For example, the

droplet size spectrum of stratiform cloud is relatively narrow and the reflectivity is nearly uniform. In cumulonimbus cloud, the core region features large droplet sizes and high water contents, whereas the marginal region features small droplet sizes and large spectral widths. These differences are therefore evident in the radar reflectivities. Hence, the magnitude and distribution of reflectivity factors are key information for cloud type identification.

Once cloud clusters have been identified, we can derive parameters that reflect cloud layer height and cloud morphology, as well as the distribution of reflectivity. Based on these parameters, a fuzzy logic algorithm is established to identify cloud type. The parameters (listed in Table 2) include average reflectivity factor intensity (Z_{ave}), orientation of ellipse long axis (θ), cloud base height (CB), cloud thickness (CT), presence/absence of precipitation (BP), ratio of horizontal to vertical extent (R_{HV}), maximum intensity of echo (Z_{max}), and the standard variance of intensities (Z_{std}). The orientation of the ellipse long axis (θ) represents the angle between the long axis and the horizontal after fitting the cloud cluster with an ellipse, and is used to differentiate horizontally and vertically distributed cloud. The standard variance of intensities (Z_{std}) represents the standard variance of reflectivity factors in the cloud cluster, indicating the homogeneity of the distribution of reflectivity factors.

The outputs of the fuzzy logic algorithm are eight cloud types: stratus (St), stratocumulus (Sc), cumulus (Cu), cumulonimbus (Cb), nimbostratus (Ns), altostratus (As), altocumulus (Ac), and high cloud.

3.2.3 Fuzzification

According to the physical features of each cloud type, a corresponding membership function is derived; the function parameters are listed in Table 3. We use typical parameter values in this study, although the parameter configuration can be modified according to geographical region and season. In addition, input parameters can be given appropriate weightings. As cloud base height and cloud thickness are critical cloud features, they are given higher weightings. Given that millimeter-wave cloud radar is susceptible to attenuation by precipitation as well as Mie scattering by large particles, the two relevant parameters, intensity mean and its standard variance, are given lower weightings. The weighting given to the orientation of the ellipse long axis is lower still, given that the detection range of millimeter-wave radar is limited and the potential for partially covered echoes. In identifying high-level cloud, cloud base height is the most important parameter.

Using the parameters listed in Table 3, different membership functions can be designed. The inputs (i) to the algorithm are the eight variables, and outputs (j) are the eight cloud types; thus, there are 64 membership functions (F_{ij}). Using function F_{ij}, the probability that input i belongs to type j can be calculated. For a set of eight inputs, the probability (P_j) of belonging to type j is

$$P_j = \sum_{i=0}^{8} P_{ij} \times W_i, \tag{2}$$

where W_i is the weighting of input i. The final cloud type is that corresponding to the largest value of P_j.

3.2.4 Accuracy of the algorithm

As is the case with human visual observation, the classification criteria of this study rely on the appearance of cloud, which is highly subjective. Hence, it is not possible to determine whether the derived cloud type is correct. The lack of reference data limits the quantitative validation of the identification algorithm. Following Wang and Sassen (2001), we compared identified cloud types with those from human visual observations. Human observers classify clouds based on their visual appearance and approximate cloud height. Observers with knowledge of radar meteorology can also classify clouds based on echo intensity and shape, especially the heights of the echo base and top in radar RHI images. In the present study, an experienced observer was asked to verify the results obtained using the classification algorithm. A total of 606 radar images taken in 2016 and 2017 were checked, and the comparison results are presented in Table 4. We note

Table 2 Input variables of the fuzzy logic algorithm

Variable	Physical meaning
Z_{ave}	The average intensity among all effective grids within cloud cluster
θ	The angle between long axis and horizontal direction after fitting cloud cluster boundary points with an ellipse
CB	The mean height of the cloud base
CT	The mean thickness of cloud cluster
BP	Precipitation is present or not according to cloud base height and intensity distribution of reflectivity factors
R_{HV}	The ratio of maximum horizontal extent to maximum vertical extent of cloud cluster
Z_{max}	The maximum of reflectivity factors within cloud cluster
Z_{std}	The standard variance of reflectivity factors among all effective grids within cloud cluster

Table 3 Fuzzification parameters for the eight algorithm inputs

	Z_{ave}		θ		CB		CT		BP		R_{HV}		Z_{max}		Z_{std}	
	m	a	m	a	m	a	m	a	m	a	m	a	m	a	m	a
St	−10	5	0	8	500	500	1000	1000	0.5	0.5	15	15	−5	15	3	3
Sc	−5	6	0	25	1000	700	1200	900	0.5	0.5	15	5	0	15	5	5
Cu	−5	8	90	40	1100	800	1500	1000	0.5	0.5	2	2	5	15	5	5
Cb	5	10	90	20	1100	500	12000	7000	1	0.5	3	3	27	8	12	5
Ns	0	5	0	40	1500	1500	6500	3000	1	0.5	4	2	22	10	5	5
As	−10	4	0	10	3500	1500	3000	2500	0	0.5	15	15	−5	10	3	3
Ac	−5	5	90	40	4000	2000	1400	700	0	0.5	2	2	0	10	5	5
High cloud					9000	3000										
Weight	0.5		0.3		2		1.5		1		1		1.2		0.5	

that there may be more than one cloud cluster in a radar image. Cloud type classifications from the algorithm are largely in accordance with those from the observer. Agreement for each cloud type is greater than 70% and the average agreement for all types is 82.1%. Relatively low agreement values were obtained for Sc and Ns cloud. The low agreement for Sc cloud might reflect the small sample volume, and that for Ns cloud is due in part to 51 of the 253 images being classified as St cloud by the observer. In the algorithm, the major difference between membership parameters for Ns and St is cloud thickness. It is possible that the observer thought St cloud had thicknesses that exceeded the range selected in the algorithm, and therefore identified thinner Ns cloud with low average reflectivity as St cloud. Despite this discrepancy, the results indicate that the algorithm performs well in cloud classification.

4 Case study and results

Typhoon Khanun (1720) made landfall in Xuwen (20.5°N, 110.2°E), Guangdong Province, China at 19:25 UTC on October 15, 2017. According the radar mosaic images (figures omitted), there was no cloud over the site when the typhoon made landfall. South-east of the radar site, a small isolated block of echo was present, located at the far end of one spiral band of the typhoon. Sequential radar images indicate that the isolated echo was moving to the north-west. At 0000 UTC on October 16, cloud moved over the radar site and produced rain. By 0100 UTC, the rain had stopped as the typhoon weakened. During this 1-h period (i.e., between 0000 and 0100 UTC), the cloud type changed rapidly. Radar RHI data for this period were used to identify cloud types and analyze their change over time.

Figures 1–3 show radar RHI images and cloud-identification results for 0000–0100 UTC on October 16, 2017. We show two images with similar radar azimuth angles to clearly demonstrate the change in cloud type. The images at 00:14:26 UTC (top) and 00:22:56 UTC (bottom), with the same azimuth of 138°, are shown in Fig. 1. The echoes in the two images were moving toward the radar. Radar reflectivity data are shown in the left part of the figures, with the identified cloud clusters overlapping. The borders of cloud clusters are indicated by red dotted lines, and the cluster number is provided at the

Table 4 Contingency table comparing cloud type derived from the algorithm with that from a human observer

		Automatic classification algorithm							
		St	Sc	Cu	Cb	Ns	As	Ac	High
Observer	St	158	3	1		51	21		
	Sc	16	10	8		5	5	2	
	Cu			49	1	3			
	Cb			1	12	5			
	Ns				2	189			
	As	5	1	2		10	159	9	
	Ac	3					12	58	
	High							1	92
Agreement		86.8%	71.4%	80.3%	80.0%	74.7%	80.7%	81.7%	100%

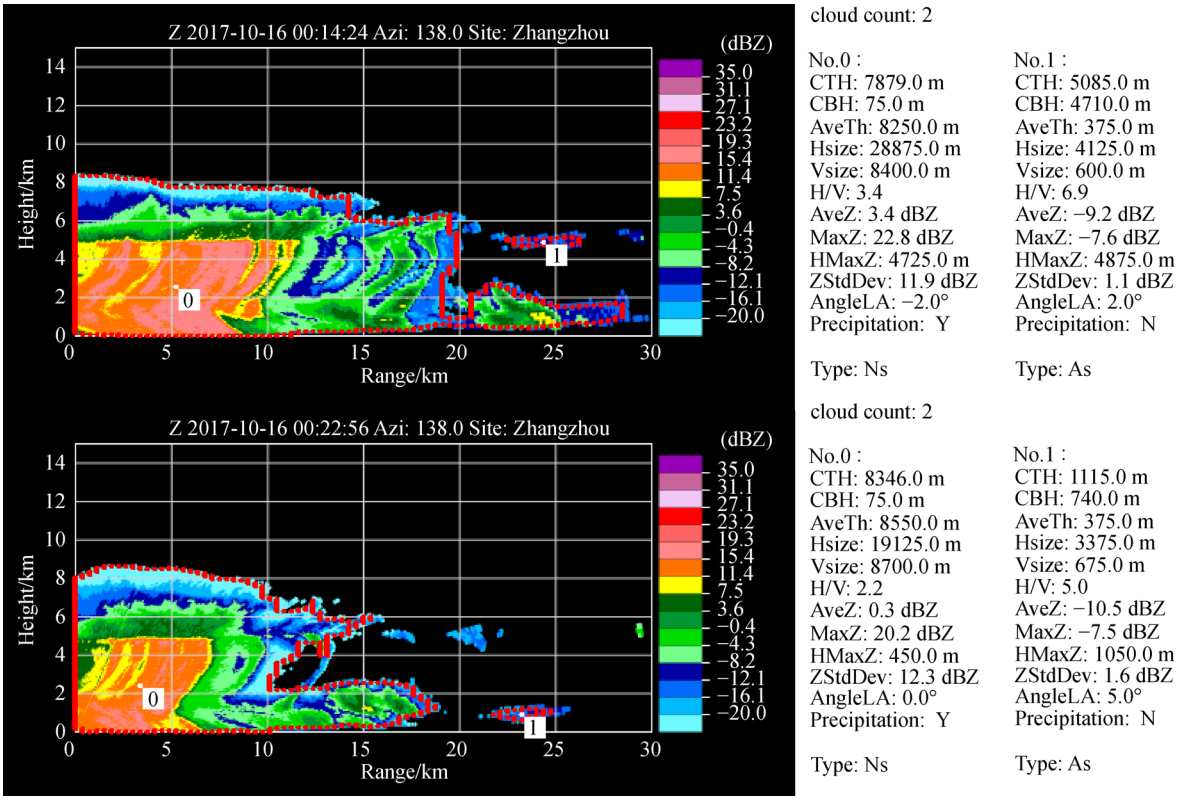

Fig. 1 Radar RHI image and identification results at 00:14:26 UTC (top) and 00:22:56 UTC (bottom) on October 16, 2017. The borders of cloud clusters are indicated by red dotted lines, and the cluster number is provided at the centroid of each cloud cluster.

centroid of each cloud cluster. The characteristics of the identified cloud clusters and cloud types are stated in the right of each figure. At 00:14:26 UTC, the main part of the echo was within the 20 km range, had a maximum reflectivity of over 20 dBZ, its base reached the ground (indicating the presence of precipitation), and its top exceeded 8 km height. Outside the 20 km range, a weaker echo, connected with the main echo, was present below 2 km height. A layer of thin cloud was present at ~5 km height. The algorithm identified these features as Ns and As cloud, respectively. The image at 00:22:56 UTC is similar to that at 00:14:26 UTC, except that the size and intensity of the clouds had decreased. The low-level echo at 20 km range had separated from the main echo and was identified as St cloud. The thin cloud that had existed at 5 km height further dissipated and was not recognized by the algorithm. The main part of the cluster was still identified as Ns cloud. The sequential images show that the cloud was weakening as it moved toward the radar site.

Radar images and cloud-identification results for 00:18:05 UTC and 00:59:12 UTC are shown in Fig. 2. The images were obtained with azimuth angles of 336° and 346.9°, respectively, and show the echo moving away from the radar site. Cloud in the first image extends to the ground and was identified as Ns. In the second image, the cloud does not extend to the ground and the center of the strong echo was higher. The main part of this cluster was identified as Cu cloud.

Figure 3 shows radar images and cloud-identification results for 00:20:26 UTC (top) and 01:01:35 UTC (bottom). The images were obtained at azimuth angles of 245° and 243°, respectively, with the echo moving toward the radar. In the first image, the cloud extended to the ground, its shape was intact, and cloud top was at a height of ~7 km. The cloud was identified as Ns. In the later image, there were three main echo regions. The two cloud clusters with larger areas and lower bases were identified as St and Cu, respectively, and the weaker echo at around 6 km height was identified as high cloud.

The above cloud-identification results show that RHI data obtained at a range of azimuth angles during the period 0000–0100 UTC clearly reveal the vertical structure of the cloud. The cloud-identification results obtained using the algorithm are consistent with the typical characteristics of the cloud types. The sequential detections and identifications reflect changes in cloud type during this short precipitation period, and provide useful information for analysis of the typhoon's evolution.

5 Conclusions

As a basic property of cloud, accurate identification of cloud type is useful in short-term forecasting of the

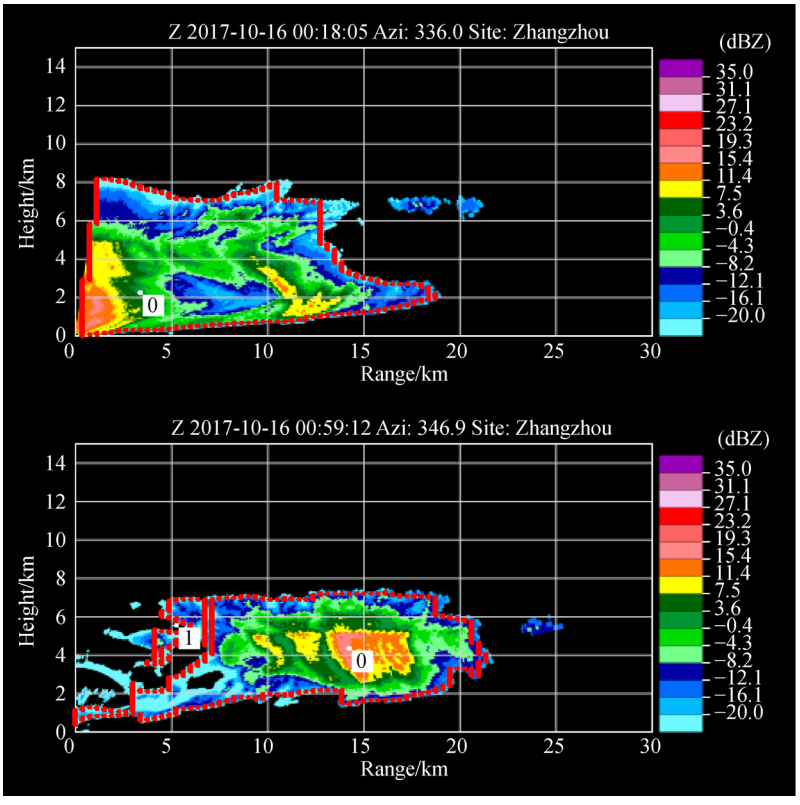

Fig. 2 As in Fig. 1, but for 00:18:05 UTC (top) and 00:59:12 UTC (bottom).

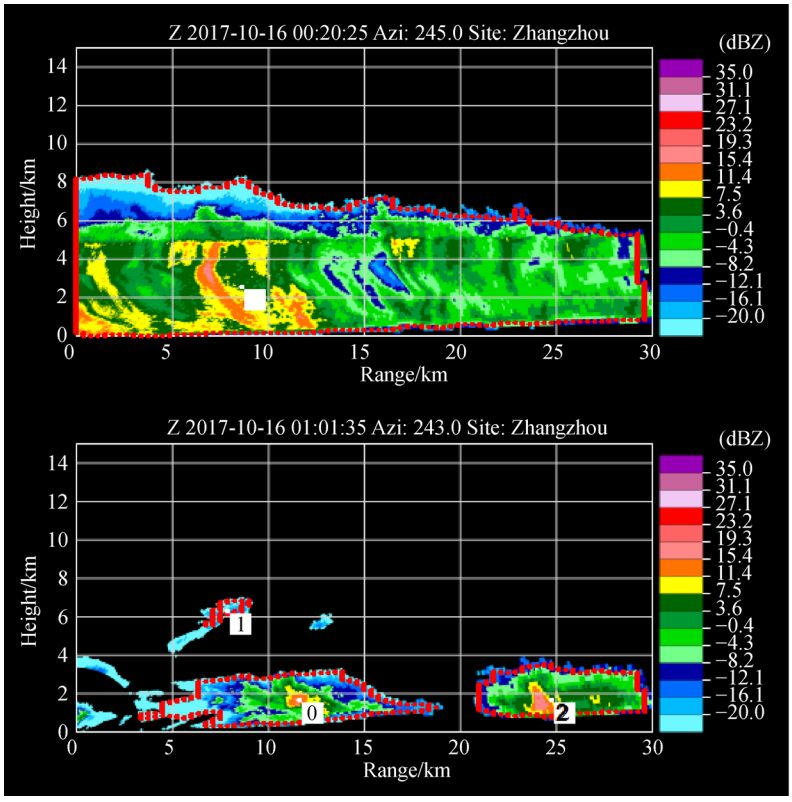

Fig. 3 As in Fig. 1, but for 00:20:26 UTC (top) and 01:01:35 UTC (bottom).

evolution of typhoons that make landfall. Furthermore, cloud type is a common target for operational observations in aviation meteorological services. Human visual observation remains the main approach to cloud classification in operational aviation meteorological services. With the aim of improving meteorological operations and typhoon forecasting, a fuzzy logic algorithm was established to identify cloud physical features and their characteristics in millimeter-wave cloud radar RHI data. The algorithm can identify eight cloud types: stratus, stratocumulus, cumulus, cumulonimbus, nimbostratus, altostratus, altocumulus and high cloud.

Compared with the common fixed upward detection mode, RHI data from millimeter-wave radars can be used to obtain cloud profile information that is better suited to the analysis of cloud type characteristics. Consequently, we have developed a cloud identification algorithm based on RHI data. In addition to typical parameters such as cloud base height, cloud thickness, and the ratio of horizontal to vertical extent, parameters that reflect cloud morphology and distribution characteristics of reflectivity factors are inputted to the algorithm, leading to improved cloud identification. Moreover, the weighting of parameters can be set according to millimeter-wave cloud radar characteristics. These input parameters are available from radar data and are therefore not dependent on other data sources. This makes the algorithm independent and readily applied in various applications. A comparison of cloud type from the algorithm and a human observer for 606 radar images shows good agreement (82.1%) when averaged over all cloud types. The identification algorithm proposed in this study provides a feasible scheme for automatic identification of cloud type.

The algorithm was applied to classify cloud type at the Zhangzhou radar site during the period when typhoon Khanun made landfall. Temporal changes in cloud type were revealed in sequential radar data, from which we observe a clear process of typhoon weakening. This case study shows that application of the cloud-type identification algorithm to sequential RHI data from millimeter-wave cloud radar yields useful information for the analysis of typhoon evolution.

Acknowledgements This work was supported by the National Natural Science Foundation of China (Grant No. 41675029), the National Basic Research Program of China (No. 2013CB430102).

References

Chu X, Geerts B, Xue L, Pokharel B (2017). A case study of cloud radar observations and large-eddy simulations of a shallow stratiform orographic cloud, and the impact of Glaciogenic Seeding. J Appl Meteorol Climatol, 56(5): 1285–1304

Delgadillo R, Voss K J, Zuidema P(2018). Characteristics of optically thin coastal florida cumuli derived from surface-based lidar measurements. J Geophys Res D Atmospheres, 123(18): 10,591–10,605

Han L, Fu S, Zhao L, Zheng Y, Wang H, Lin Y (2009). 3D convective storm identification, tracking, and forecasting—an enhanced TITAN algorithm. J Atmos Ocean Technol, 26(4): 719–732

Jet Propulsion Laboratory (2012). Level 2 Combined Radar and Lidar Cloud Scenario Classification Product Process Description and Interface Control Document

Kollias P, Clothiaux E E, Miller M A, Albrecht B A, Stephens G L, Ackerman T P (2007). Millimeter-wavelength radars: new frontier in atmospheric cloud and precipitation research. Bull Am Meteorol Soc, 88(10): 1608–1624

Kumar A, Singh N, Singh A (2019). Observations on the distribution of clouds over northern India using joint CloudSat and CALIPSO measurements. Remote Sens Lett, 10(6): 590–597

Küchler N, Kneifel S, Löhnert U, Kollias P, Czekala H, Rose T (2017). A W-Band radar-radiometer system for accurate and continuous monitoring of clouds and precipitation. J Atmos Ocean Technol, 34 (11): 2375–2392

Li X, Zheng X, Zhang D, Zhang W, Wang F, Deng Y, Zhu W (2018). Clouds over east asia observed with collocated cloudSat and CALIPSO measurements: occurrence and macrophysical properties. atmosphere, 9(5): 168

Liu H, Chandrasekar V (2000). Classification of hydrometeors based on polarimetric radar measurements: development of fuzzy logic and neuro-fuzzy systems, and *in situ* verification. J Atmos Ocean Technol, 17(2): 140–164

Rémillard J, Fridlind A M, Ackerman A S, Tselioudis G, Kollias P, Mechem D B, Chandler H E, Luke E, Wood R, Witte M K, Chuang P Y, Ayers J K (2017). Use of cloud radar Doppler spectra to evaluate stratocumulus drizzle size distributions in large-eddy simulations with size-resolved microphysics. J Appl Meteorol Climatol, 56(12): 3263–3283

Sassen K, Wang Z (2008). Classifying clouds around the globe with the CloudSat radar: 1-year of results. Geo Res Lett, 35: L04805

Stephens G L, Vane D J, Boain R J, Mace G G, Sassen K, Wang Z, Illingworth A J, O'connor E J, Rossow W B, Durden S L, Miller S D, Austin R T, Benedetti A, Mitrescu C (2002). The cloudsat mission and the A-train. Bull Am Meteorol Soc, 83(12): 1771–1790

Wang Z, Sassen K (2001). Cloud type and macrophysical property retrieval using multiple remote sensors. J Appl Meteorol, 40(10): 1665–1682

Wang Z, Wang Z, Cao X, Mao J, Tao F, Hu S (2018). Cloud-base height derived from a ground-based infrared sensor and a comparison with a collocated cloud radar. J Atmos Ocean Technol, 35(4): 689–704

World Meteorological Organization (2017). "Observation" of Clouds Chap. 15.1 in Guide to Meteorological Instruments and Methods of Observation (WMO-No.8)

Sokol Z, Minářová J, Novák P (2018). Classification of hydrometeors using measurements of the ka-band cloud radar installed at the Milešovka Mountain (Central Europe). Remote Sens, 10(11): 1674